Proceedings of ES2008
Energy Sustainability 2008
August 10-14, 2008, Jacksonville, Florida USA

ES2008-54122

ELECTRICITY GENERATION FROM A COMPOUND PARABOLIC CONCENTRATOR COUPLED TO A THERMOELECTRIC MODULE

Chigbo A. Mgbemene[1]*

John Duffy[2], Hongwei Sun[2], Samuel O. Onyegegbu[1]

Abstract

Generating electricity from the sun using a combination of a compound parabolic concentrator (CPC) and a thermoelectric module (TEM) has been studied. The system was modeled, analyzed and tested. The model equations and the methodology used for the demonstration are presented and experimentally validated. The experimental setup comprised a manually fabricated CPC placed on a commercially available TEM. The results showed that the combination can generate and sustain enough power for a small appliance. It was also shown that there is enough dissipated heat from the system which could be harnessed for additional uses. The cost is still high, about $35/Wp, but if credit is given for the thermal energy the initial cost goes down.

Nomenclature

A	Area [m^2]
CR	Concentration ratio
h	Heat transfer coefficient [W/m^2K]
I	Electrical current [A]
I_s	Solar radiation [W/m^2]
K	Thermal conductance [W/K]
L	Thermoelement length [m]
N_{th}	Number of thermoelements
P	Power [W]
q	Heat flow [W]
R	Electrical resistance [Ω]
S_{in}	Concentrated solar radiation [W/m^2]
T	Temperature [K]
U_L	Heat loss coefficient [W/m^2K]
V	Voltage [V]
V_a	Velocity of air [m/s]
Z	Figure of merit

Greek Symbols

α	Seebeck coefficient [V/K]
ΔT	Temperature difference [K]
ε	Emittance
η	Thermal efficiency
θ	Acceptance angle [^{o}]
λ	Thermal conductivity [W/mK]
ρ	Electrical resistivity [Ω-m]
σ	Stefan-Boltzmann constant [W/m^2K^4]

Subscripts

a	Relating to the surrounding ambient air
c	Cold side of thermoelectric
h	Hot side of thermoelectric
hs	Heat sink
m	Thermoelectric module
n	n-type thermoelement
p	P- type thermoelement
th	Thermoelement
w	Water
L	Loss, load

*Corresponding author. Tel.: +234-803-4263781
E-mail address: chigbomgbemene@yahoo.com

[1]Department of Mechanical Engineering,
University of Nigeria, Nsukka, Enugu State Nigeria

[2]Department of Mechanical Engineering,
University of Massachusetts, Lowell,
Massachusetts 01854 USA

1. INTRODUCTION

1.1 Thermoelectric generators

Thermoelectric generators (TEG) convert heat energy directly to electricity. They have the advantage of being able to operate from a low grade heat source as well as from a high grade heat source. This is a great advantage because this makes them appropriate to be used for waste heat conversion into

electricity and also for harnessing electricity from the sun [1, 2].

A thermoelectric generator is a unique solid state energy generator. It has no moving parts and is very reliable and environmentally friendly. It consists of an array of n- and p-semiconductor thermoelements connected electrically in series and thermally in parallel. They are joined at the ends and are sandwiched between two ceramic insulators which also serve as their foundation and electrical insulator. This arrangement forms a thermoelectric module (TEM). The thermoelectric module is then sandwiched between a heat source and a heat sink creating a temperature difference between the module's hot surface and the cold surface. As a result of this temperature difference, a current flows through an external load resistance. An electrical power is generated as long as the temperature difference is maintained between the two surfaces. The module in this form is known as a thermoelectric generator (TEG). A basic arrangement is as shown in the Fig. 1.

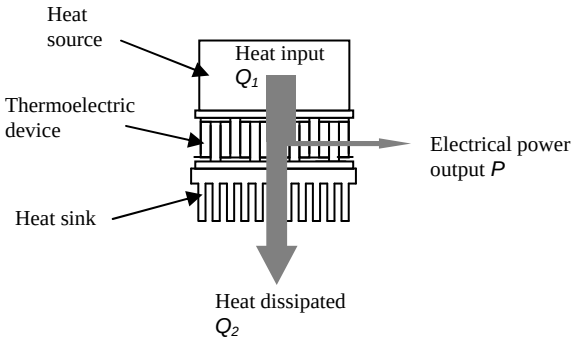

FIG. 1. THE BASIC ARRANGEMENT FOR THERMOELECTRIC POWER GENERATION.

The thermoelectric generators make no noise when they run and if any noise at all, it will come from the fan (for the air cooled system). For water cooled system, there is practically no noise at all. The TEG's are modular and so increments in power output can be achieved by simply adding more modules to the system

The TEM has low conversion efficiency. The low conversion efficiency has been a major factor limiting their application in electrical power generation. It has also restricted their use to specialized situations where reliability is a major consideration [3, 4]. It is not surprising though because the TEM is a thermal device which operates between two temperature regimes, therefore the Carnot efficiency limits its absolute energy conversion efficiency.

Over the past four decades, improvements in the conversion efficiency have been marginal. The challenge has been the development of thermoelectric materials with an improved dimensionless figure of merit ZT (T is the absolute temperature, $Z = \alpha^2/\rho\lambda$. α^2/ρ is referred to as the electrical power factor) [5]. The thermoelectric material commonly in use now is the Bismuth Telluride Bi_2Te_3 and currently, the best thermoelectric material possesses a maximum value of ZT approximately 1. Although a number of new promising approaches in improving ZT have been proposed, these are yet to be realized in practice [5].

Several other parameters also affect the power output and the conversion efficiency of the TEG; these have been studied by Rowe, Min, Chin, and others [3, 6, 7, and 8]. Amongst these parameters, the temperature difference has the greatest effect on the power output. This is quite fortunate because there is an abundance of waste heat sources which can be harnessed for power generation. However, the quality of the heat source is important. High temperature energy sources result in higher power output and higher efficiencies because of the high temperature differences, ΔT's [7, 9]. But a combination of even a low grade heat source and a good heat sink can result in a good temperature difference and hence, a substantial power output [10].

Ideally, a large power output can be generated while dissipating only a little quantity of heat to the sink, but this is not so in the actual case. Rather over 95% of the heat input is dissipated to the heat sink while the rest is converted into power. This large dissipated quantity of heat can still be useful if harnessed also [5].

1.2 Compound parabolic concentrators (CPC)

The sun is a good source of low grade heat energy and its energy comes free. Chen, [11], and Khattab and Shenawy [12] have shown that meaningful power output can be obtained from the TEG driven by the solar energy. The solar energy can be utilized more efficiently when it is concentrated. This can be done using solar concentrators. There are different types of solar concentrators [13, 14] but the type to be used for this work is the compound parabolic concentrator (CPC). The CPC is a concentrator with each side a parabola as shown in Fig. 2.

The analysis of the CPC can be found in [13, 14 and 15]. The CPC is most useful as linear or trough-type concentrators which are two-dimensional in nature, but for this work, a three-dimensional CPC is more suitable.

This work aims to demonstrate the concept that the 3D CPC can be suitable in harnessing the solar energy and generating power when coupled to a TEM. It also aims at showing that the dissipated heat is large enough to be harnessed too. This latter part is hoped to be achieved by using water as the cooling fluid in the heat sink. The water, which gets preheated, could then be channeled for space heating and/or domestic hot water use, thereby saving energy and reducing energy costs.

The objective of this work is to estimate the feasibility, efficiency, and cost effectiveness of combining a small CPC and a TEM to produce electrical and thermal energy from the sun. The approach is to develop a relatively straightforward mathematical model and then to build a prototype and make experimental measurements consistent with a preliminary proof-of-concept evaluation.

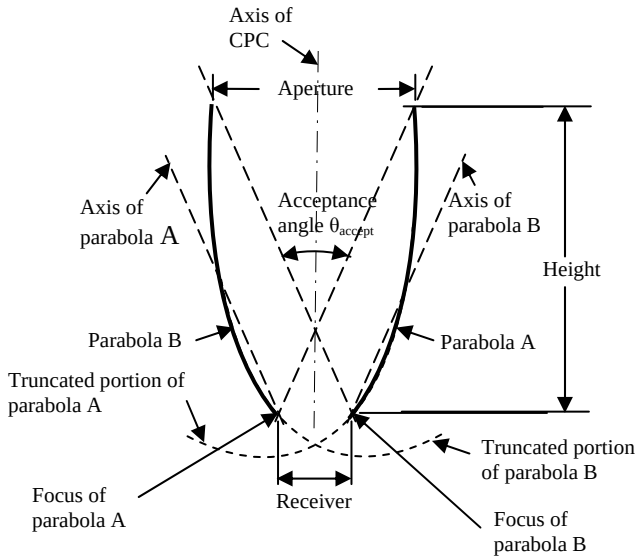

FIG. 2. CROSS SECTION OF A NONTRUNCATED COMPOUND PARABOLIC CONCENTRATOR (CPC) [14]

Analyses of the CPC, the basic equations of the TEM together with an energy balance of the TEM were used to develop a mathematical model to simulate the performance of the CPC/TEM system. The model was developed for a water cooled system but the generator performance was validated with an air-cooled system for which actual experimental results were obtained.

2. THEORETICAL ANALYSIS OF THE SYSTEM

2.1 Evaluation of the CPC

The CPC is here evaluated to determine the upper limit of the concentration and also to establish its operating temperature limits. As the CPC was truncated, it is necessary to determine the effective height of truncation for this application.

According to [13, 15], the geometrical concentration ratio of the CPC *CR* is given as

$$CR = \frac{A_a}{A_r} \tag{1}$$

where A_a = aperture area
A_r = receiver area.

Applying the second law of thermodynamics to the concentrator, the theoretical maximum possible concentration ratio obtainable from it can be evaluated to be

$$CR_{\max,3D} = \frac{1}{Sin^2 \frac{1}{2}\theta_{\max}} \tag{2}$$

where θ_{max} = maximum acceptance angle

From the above equation, the optical limits of concentration can also be obtained. Note $CR \le CR_{max}$.

The second law of thermodynamics also prescribed the operating temperature limits of the concentrator [15]. If the heat loss due to radiation is assumed the dominant loss factor, the maximum receiver temperature T_r can be found to be

$$T_r = T_s\left[(1-\eta_c)\tau\frac{\alpha_s}{\varepsilon_r}\frac{CR}{CR_{\max}}\right]^{\frac{1}{4}} \tag{3}$$

where T_s = effective temperature of the sun
τ = overall transmittance of the concentrator
α_s = solar absorptance of the collector-absorber plate surface
ε_r = emittance of the receiver surface
η_c = fraction of energy absorbed at the receiver that is delivered to the TEM thermoelements.

η_c is given as

$$\eta_c = \eta_p - \frac{U_c(T_c - T_a)}{I_s CR} \tag{4}$$

where η_p = optical efficiency of the concentrator
U_c = overall concentrator heat loss coefficient
T_c = collector plate temperature

The truncation height of a 2D CPC can be determined as given in [13], but the method cannot be applied to 3D CPCs. For this experiment, a convenient truncation height was chosen. It was truncated to a height-to-aperture ratio of 1. The truncated height was 110mm corresponding to a 70% truncation. For a chosen θ_{max} of 28°, the untruncated values of CR_{max} and *CR* obtained were 17:1 and 10:1 respectively.

Truncation affects the performance of the CPC though not greatly, therefore, the actual concentration ratios obtained from the experimental CPC are less than the calculated values.

2.2 Evaluation of the TEM

Rowe and Min in [3] evaluated the generating performance of the TEM in terms of its power output, conversion efficiency and reliability. They further investigated the potential for improving its performance based on the power-per-area, cost-per-watt and manufacture quality factor. They evaluated several commercially available modules. They presented that when consideration is taken of the effects of thermal and electrical resistances, the power output per unit area ($p=P/N_{th}A_{th}$), and the conversion efficiency of the module are given by,

$$P = \frac{\alpha^2}{2\rho}\frac{N_{th}A_{th}\Delta T^2}{(l+n)(1+2rl_c/l)} \tag{6}$$

$$\phi = \left(\frac{T_h - T_c}{T_h}\right)\left\{\left(1 + 2rl_c/l\right)^2\left[2 - \frac{1}{2}\left(\frac{T_h - T_c}{T_h}\right) + \frac{4}{ZT_h}\left(\frac{l+n}{l+2rl_c}\right)\right]\right\}^{-1} \quad (7)$$

where φ = conversion efficiency
l_c = thickness of the insulating layers in the TEM
n and r = contact parameters of a given module

$n = \rho_c/\rho$ and $r = \lambda/\lambda_c$

where ρ_c = electrical contact resistivity
λ_c = thermal contact resistivity

From Eqs. (6) and (7) the conversion efficiency can be estimated together with the corresponding maximum power output. The manufacture quality factor F can be obtained by rewriting Eq. (6) as,

$$P = F.N_{th}\Delta T^2\left(\frac{\alpha^2}{2\rho}\right)\left(\frac{A_{th}}{l}\right) \quad (8)$$

where

$$F = \frac{1}{\left(1+\frac{n}{l}\right)\left(1+\frac{2rl_c}{l}\right)^2} \quad (9)$$

It can be seen that the contact resistances seriously affect the generating performance of the TEM.

The commercially available module by Melcor [16] used for this experiment has similar properties to the ones used in [3].

2.3 The system model

The arrangement of the setup for this experiment is shown in Fig. 3. It may also be expressed as a one-dimensional equivalent thermal network as in Fig. 4.

When a constant heat flux is applied to one side of the thermoelectric generator and the other side is kept at a lower temperature, an electrical power output is obtained. Traditionally, thermoelectric systems are analyzed using the thermal resistance model, so in this case, an equation for this output power can be derived by carrying out an energy balance of the system's thermal resistance network - Fig. 4(b). This equation depends on the thermoelement geometry and material parameters as well as on temperature difference across the TEG.

The energy balance at the nodes from Fig. 4(b) may be written as:

At node 1:

$$q_3 = S_{in}A_m - q_L \quad (10)$$

$$S_{in} = \eta_{CPC} I_S CR \quad (11)$$

$$q_L = \left[\varepsilon_1\sigma\left(T_1^4 - T_a^4\right) + h_a\left(T_1 - T_a\right)\right]A_m \quad (12)$$

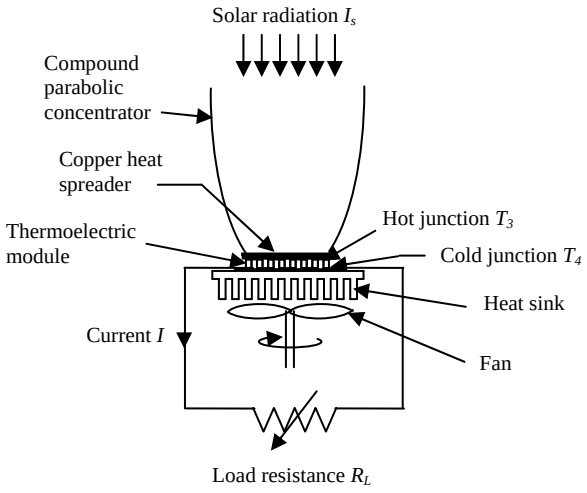

FIG. 3. THE ARRANGEMENT OF THE CPC/TEM THERMOELECTRIC GENERATOR.

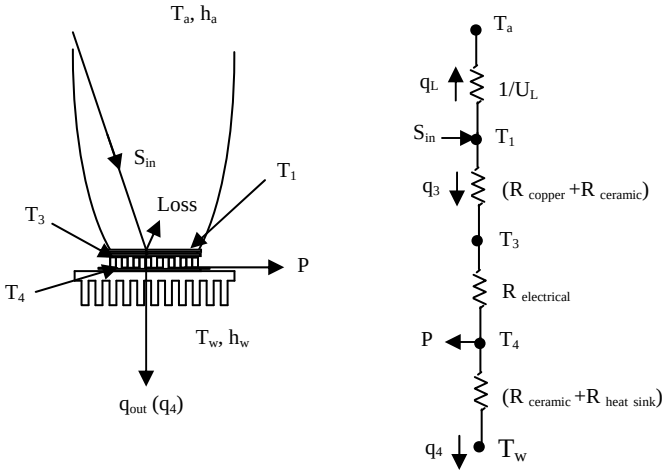

FIG. 4. (A) THE SCHEMATIC DIAGRAM OF THE TEG. (B) THE ONE-DIMENSIONAL EQUIVALENT THERMAL NETWORK.

At node 3(hot junction):

$$q_3 = \frac{T_1 - T_3}{R_{copper} + R_{ceramic}} \quad (13)$$

At node 4(cold junction):

$$P = q_3 - q_4 \quad (14)$$

$$q_4 = \frac{T_4 - T_w}{R_{ceramic} + R_{hs} + R_{convection}} \quad (15)$$

When heat conduction effect and internal irreversibility, such as Joule's heating effect due to the electrical current and Peltier heating/cooling effect are taken into consideration, the basic set of heat balance equations at the hot and cold junctions can then be given as:

$$q_h = \alpha I T_h + K(T_h - T_c) - 0.5 I^2 R \quad (16)$$

$$q_c = \alpha I T_c + K(T_h - T_c) - 0.5 I^2 R \quad (17)$$

where K and R are respectively the thermal conductance and the internal electrical resistance of the thermoelectric device, and α is the Seebeck coefficient of the thermoelectric device, which according to [17] is temperature dependent. α then becomes the difference between the Seebeck coefficients of the p- and n- thermoelements at the given temperature

$$\alpha = \alpha_p - \alpha_n$$

The electrical power according to [17] is given as

$$P = I^2 R_L = \left[\frac{N_{th}(\alpha_p - \alpha_n)(T_h - T_c)}{R_L + R} \right]^2 R_L \quad (18)$$

For maximum power generation the load resistance R_L should equal the internal electrical resistance R of the TE device [18, 19].

According to [17], the thermal conductance K of a TE module is dependent on the thermoelement length L, cross-sectional area A_{th} of a single element and the effective thermal conductivity of the thermoelement material λ and is expressible as

$$K = 2N_{th} \frac{\lambda A_{th}}{L} \quad (19)$$

The internal electrical resistance R of the module is related to N_{th}: number of thermoelement pairs, A_{th}: cross-sectional area of a single element and ρ: average electrical resistivity of thermoelement material as

$$R = 2N_{th} \frac{\rho L}{A_{th}} \quad (20)$$

Combining Eqs. (10) to (20) for a maximum power output situation and where $T_h = T_3$ and $T_c = T_4$, the model equations for the power output and heat flow are obtained as

$$P = \frac{N_{th} A_{th} \left[(\alpha_p - \alpha_n)(T_3 - T_4) \right]^2}{8\rho L} \quad (21)$$

$$q_3 = \frac{N_{th} A_{th} (\alpha_p - \alpha_n)^2 (T_3 - T_4) T_3}{4\rho L} - \frac{N_{th} A_{th} \left[(\alpha_p - \alpha_n)(T_3 - T_4) \right]^2}{16\rho L} + 2N_{th} \frac{k}{L} A_{th} (T_3 - T_4) \quad (22)$$

$$q_4 = \frac{N_{th} A_{th} (\alpha_p - \alpha_n)^2 (T_3 - T_4) T_4}{4\rho L} + \frac{N_{th} A_{th} \left[(\alpha_p - \alpha_n)(T_3 - T_4) \right]^2}{16\rho L} + 2N_{th} \frac{k}{L} A_{th} (T_3 - T_4) \quad (23)$$

The output current is given as

$$I = \frac{A_{th}(\alpha_p - \alpha_n)(T_3 - T_4)}{4\rho L} \quad (24)$$

The output voltage can then be obtained from the simple relation of

$$P = IV \quad (25)$$

The thermal efficiency η of the system is given as

$$\eta = P / q_3 \quad (26)$$

The system overall efficiency η_o is given as

$$\eta_o = p / I_s \quad (27)$$

2.4 The Experimental setup

The compound parabolic concentrator, which was manually designed and fabricated, was attached to a thin copper heat spreader which in turn was lapped unto a Melcor thermoelectric module HT 4-12-40 with 127 pairs of thermoelements and a maximum specified temperature of 200°C (473K) [16]. These formed the hot side of the TEG. The other surface of the TEM was coupled to a heat sink to form the cold side of the TEG. A Nidec TA350DC 12V DC cooling fan was then attached to the heat sink. The fan had a flow rate of 56CFM. If the setup were to use water for cooling, then the heat sink would instead be placed in a water jacket through which cold water would be passed. The setup is as shown in Fig. 5.

T-type thermocouples were attached to both the upper and lower surfaces of the TEG to measure the surface temperatures. For measuring the properties of the air, a Kestrel 3000 digital meter capable of measuring air velocity, temperature and humidity was used. Digital multimeters (Fluke 3 1/2 digit) were also used to read the current, voltage and temperature output. A CM3 pyranometer (S/N 026212) with a sensitivity of 22.31x 10^{-6} V/Wm^{-2} was used for measuring the insolation. The whole setup (Fig. 5) was then mounted on a manual solar tracker as shown in Fig. 6. The instrumentation for the experiment is as shown in Fig. 7.

FIG.5. THE EXPERIMENTAL CPC/TEM THERMOELECTRIC GENERATOR SETUP.

Detailed measurements of parameters like the thermal interface resistances between the TEM and the heat sink were neglected. Such parameters obviously come into play in a full concept evaluation. The parameters measured were just enough to establish the feasibility of the concept.

At the beginning of the experiment, separate tests were carried out to test the performance of the CPC under various conditions. One condition was when the CPC was covered with a transparent UV stabilized plastic material and another was without cover. The CPC was placed over the pyranometer such that the pyranometer was at the focal point of the CPC. The setup was then faced towards the sun and the pyranometer reading was taken.

The CPC was then coupled to the TEM and several sets of voltage, current and temperature readings were taken for different periods of the day with the sun as the heat source. These readings were only taken when the pyranometer reading indicated a maximum insolation. The average reading of each set was obtained. The cooling fan air velocity V_a, the hot and cold surface temperatures T_1 and T_4 and the ambient temperature were also measured at any period of reading.

The TEM was later subjected to a different heat source to compare the output with that of the sun as the heat source and again to know the behavior of the TEM at elevated temperatures.

The heat source used this time was the electric iron with a maximum surface temperature of 200^{o}C (473K) (though this was never reached during the experimentation). The iron was placed on the TEM to cover the whole surface and the cooling fan was turned on. The voltage, current and temperature readings were then taken at different electric iron surface temperatures.

FIG. 6. THE EXPERIMENTAL SETUP MOUNTED ON A MANUAL SOLAR TRACKER AND PLACED IN THE SUN.

FIG.7. THE INSTRUMENTATION FOR THE EXPERIMENT

2.5 Uncertainty analysis

The uncertainty in the experimental data was analyzed using the method presented by Kline and McClintock [20] on the basis of the uncertainties in the primary measurements.

If the result R is given as a function of independent variables $x_1, x_2, x_3, \ldots, x_n$, then

$$R = R(x_1, x_2, x_3, ..., x_n) \quad (28)$$

The uncertainty in the result w_R is given as

$$w_R = \left[\left(\frac{\partial R}{\partial x_1} w_1 \right)^2 + \left(\frac{\partial R}{\partial x_2} w_2 \right)^2 + ... + \left(\frac{\partial R}{\partial x_n} w_n \right)^2 \right]^{\frac{1}{2}} \quad (29)$$

where w_1, w_2, w_3, …., w_n are the uncertainties in the independent variables. The calculated uncertainties for the different parameters are shown as percentages in Table 1.

TABLE 1: CALCULATED UNCERTAINTIES FOR DIFFERENT PARAMETERS

Parameter	Uncertainty (%)
Voltage	12.30
Temperature	12.03
Heat energy	12.16
Efficiency	11.80
Power	19.00
Current	11.47

3. RESULTS AND DISCUSSION

In the setup where the CPC was covered denoted setup A, the measured pyranometer reading was 6055 W/m^2 against the 945 W/m^2 obtained from the pyranometer alone without being attached to the CPC. This 945 W/m^2 is within the range of the average normal insolation obtained in UMass Lowell, Massachusetts where the experiment was conducted. The setup where the CPC was not covered (denoted setup B) even gave a higher value of 7167 W/m^2. Other setups were tried but the setups A and B gave higher pyranometer readings. Ordinarily, it is expected that because of losses due to convection, the setup B will result in a lower temperature readings than that of A. When the CPC was covered, the cover reflected irradiation back into the atmosphere. Hence the higher value in setup B. The experiment was carried out mostly in the B setup. This gave a concentration ratio of 7.6:1 as compared to the designed concentration ratio of 10:1. This was because the CPC was truncated and manually fabricated. The surface had some defects and was uneven. These resulted in some losses due to reflection of energy back into the ambient. Nevertheless, the CPC was able to give some reasonable results.

A typical set of results can be seen from the plot of the results (Figs. 8 and 9). Plots of the values obtained from the experiment indicate an agreement with the guiding equations. A plot of the power output P versus the temperature difference ΔT is quadratic which agrees with the equation relating both of them.

It is necessary to point out that P was not measured directly but rather, was calculated from Eq. (25), but values of the current I and the voltages V generated were measured directly from the setup. The heat dissipated q_4 was not measured but was also calculated. The irradiation heat input q_3 was calculated from the temperatures measured on the hot and cold junctions of the TEM. At the same time, the pyranometer

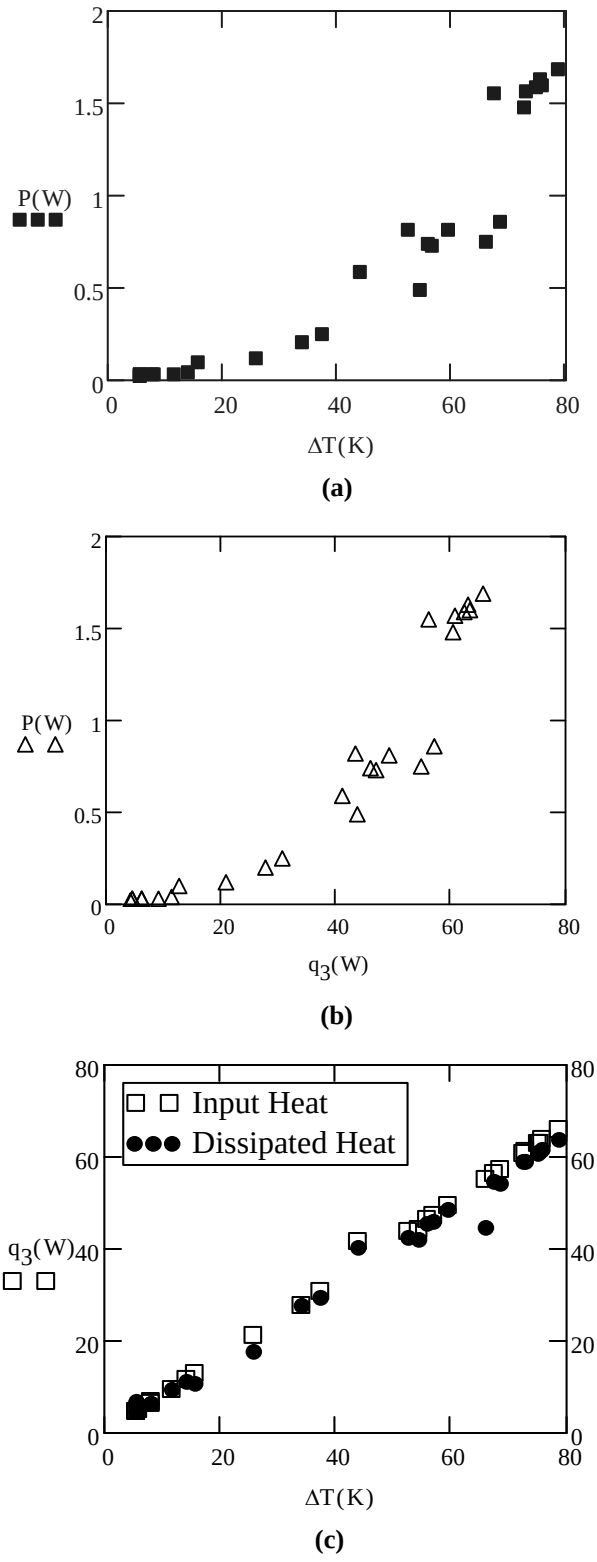

FIG. 8. PLOTS OF (A) POWER OUTPUT VERSUS TEMPERATURE DIFFERENCE. (B) POWER OUTPUT VERSUS IRRADIATION HEAT INPUT. (C) HEAT INPUT, HEAT DISSIPATED VERSUS TEMPERATURE DIFFERENCE.

reading was taken to obtain the corresponding solar irradiation. With the pyranometer reading being in V/Wm^{-2}, the voltage obtained was simply read off and then related to the pyranometer sensitivity and the unconcentrated irradiation heat was obtained. This is necessary for the estimation of the system's overall efficiency. The values used were actually average figures because the readings kept fluctuating.

From Figs. 8(a) and (b), it will be observed that as the heat input q_3 into the TEM, and the temperature difference ΔT, are increased, the power generated by the TEM increased exponentially. The heat dissipated q_4 also increased but fortunately, linearly as shown in Fig. 8(c). It could also be seen that q_4 reacts directly proportional to ΔT as shown by the linearity of their plot. This means that with an increased ΔT more power could be obtained without losing much heat exponentially to the ambient or the reservoir. It was observed from the plot of 8(c) that about 97% of heat input into the system is lost to the reservoir, but could be harnessed from the heat sink.

As stated earlier, a plot of q_4 versus q_3 is linear indicating that as q_3 is increased, q_4 also increased, but with q_3 being increased alone without an increased cooling, the heat dissipated q_4 in this case is more than that dissipated with a high ΔT. A high q_3 without cooling results in a high q_4 and a lower ΔT and therefore a lower power output. So, a higher q_3 should be matched with a high ΔT to actually lower the q_4 value. At whatever q_3, there is a consistent ratio of P to q_4 and since the q_4 is consistent and significant, it could then be harnessed for use knowing it will always occur.

From the graph of the thermal efficiency η versus heat input q_3 (Fig. 9a) and thermal efficiency η versus temperature difference ΔT (Fig. 9b); it could be observed that the thermal efficiency increases with increasing heat input and increasing temperature difference. The overall efficiency is defined (Fig. 9c) as electrical energy out relative to solar irradiation in (with the fan energy not included). This is lower than the thermal efficiency as expected but it increases with increasing solar irradiation. The limit of increase was not determined in the experiment but it is obvious that the performance of the TEM/CPC improves with higher heat throughput.

Looking at Fig. 9 (except Fig. 9c), one can note the section of the graphs which were contributed by the CPC are the lower left sections. It is now left to be shown that the CPC can be made to raise the heat quantity passed through the TEM to match or come close to that of the electric iron used for the test. The major setback in the performance of the CPC was the unevenness of the surface. The concentrator was found to be slightly off focus due to errors during fabrication. Losses due to convection also contributed to the low performance of the CPC. Insulation around the CPC with cover could help reduce the heat loss on the hot side of the TEM.

If the concentration is increased such that the ΔT's are increased to match that achieved by the electric iron, the results exhibited by the upper section of the graph would be obtained. With the CPC configuration made such that this concentration could be achieved, then it is possible to achieve this expectation.

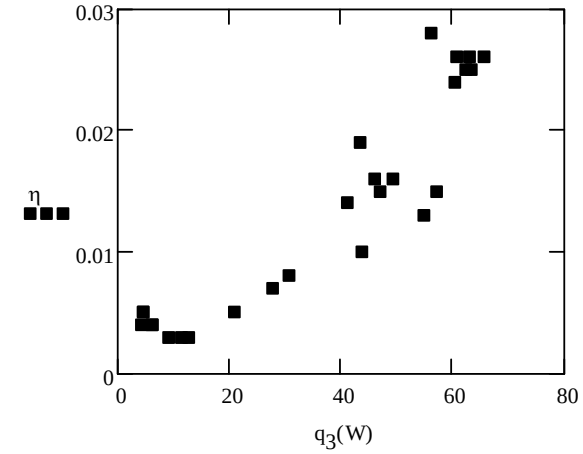

(a)

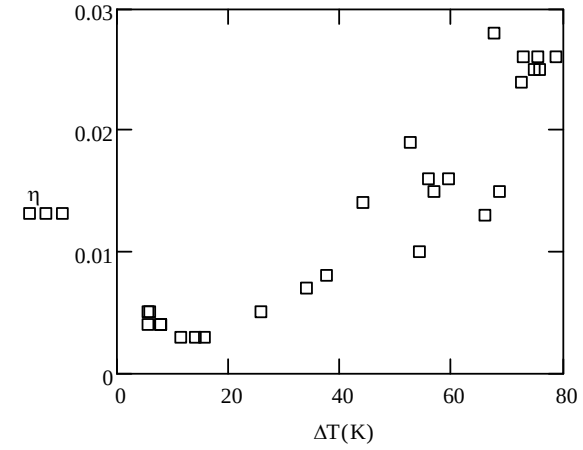

(b)

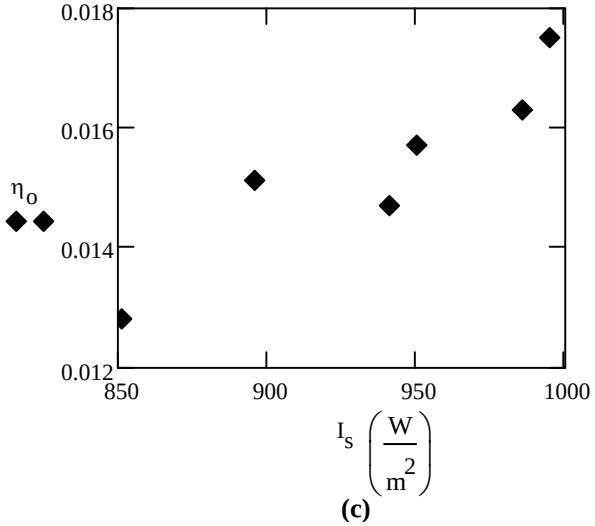

(c)

FIG. 9. PLOTS OF (A) THERMAL EFFICIENCY VERSUS HEAT INPUT. (B) THERMAL EFFICIENCY VERSUS TEMPERATURE DIFFERENCE. (C) OVERALL EFFICIENCY VERSUS SOLAR IRRADIATION.

The configuration of the CPC is such that the heat sink can accommodate two TEMs. The fan itself can accommodate four TEMs. This means four times power output from the same fan power input. However, the ratio of the concentrator's depth to the reflector aperture can become excessive and impracticable at some point. That determines the upper limit of the low grade concentration achievable from that CPC.

The fabricated concentrator concentrated the solar energy on a particular area of about 20% of the surface area of the TEM. The temperature distribution on the surface of the TEM is estimated to be as shown in Fig. 10. A copper plate, or heat spreader, was added to distribute the heat on the TEM. A black coating was also added to the heat spreader to increase absorptance. That resulted in about 20% improvement on the temperature distribution on the TEM.

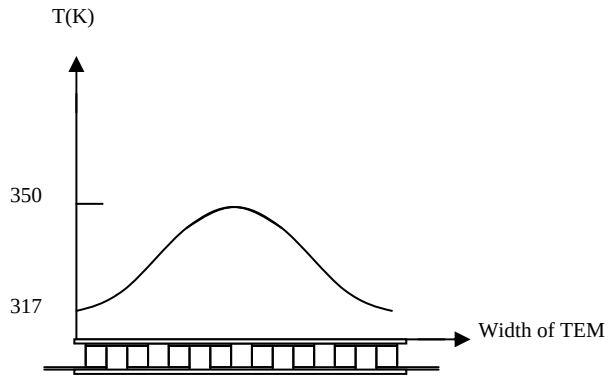

FIG. 10. TEMPERATURE DISTRIBUTION ON THE SURFACE OF THE TEM.

4. EXPERIMENTAL VALIDATION

A comparison between the predicted results from the model equations and the experimental results shows an agreement between them. This indicates that the model is sufficiently good to simulate the system performance.

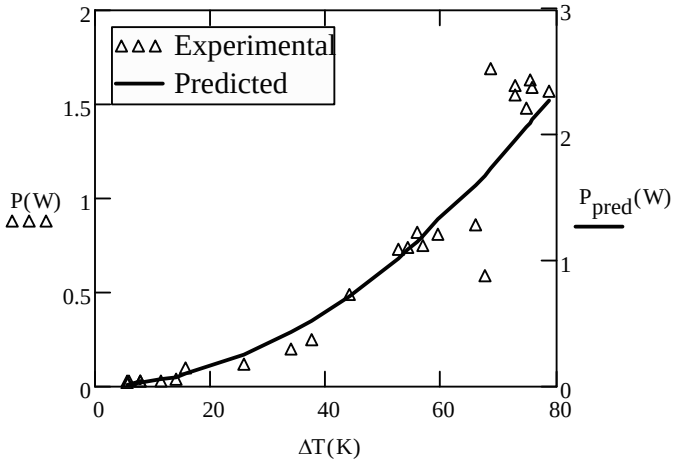

(a)

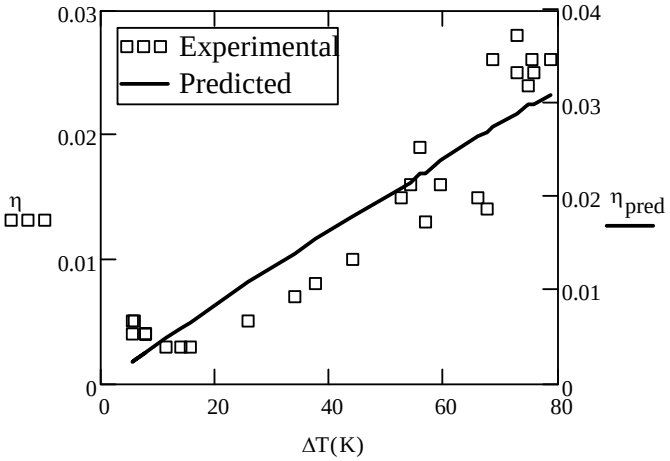

(b)

FIG. 11. COMPARISON OF DATA: PREDICTED VALUES AND EXPERIMENTAL VALUES FOR (A) POWER OUTPUT VERSUS TEMPERATURE DIFFERENCE. (B) THERMAL EFFICIENCY VERSUS TEMPERATURE DIFFERENCE

Two of the comparison plots of the data obtained from the module tests are shown in Fig. 11. The experimental data here compared well within the expected uncertainty range with the predictions of the analytical model as the other plots did. The configuration used for generating the values for Fig. 11 is that with the copper plate as the heat spreader on the TEM and no cover for the CPC.

5. CONCLUSIONS

The concept of combining a compound parabolic concentrator with a thermoelectric module to produce electricity and thermal energy from the sun was explored with a mathematical model, a simple prototype, and some preliminary experimental measurements. The measurements were consistent with the model predictions and established proof-of-concept. Efficiencies of electrical power generation reached 3% experimentally, with costs estimated at about $35/Wp. There is considerable potential to capture thermal energy for water or air heating otherwise dissipated to the atmosphere and then obviously to increase efficiency and lower cost per unit of useful energy produced. The major driving factor in the performance of the TEM/CPC system is the temperature difference across the TEM sides. Therefore, the major aim in running such a TEG would be to have a good temperature difference ΔT and a good cooling system. An idea for future analysis would be to use a TEM to help cool a photovoltaic cell in a CPC system.

REFERENCES

[1] Mastbergen, D., and Willson, B., 2005, "Generating light from stoves using a thermoelectric generator," http://www.bioenergylists.org/stovesdoc/ethos/mastbergen/Mastbergen_ETHOS_2005.pdf.

[2] Rowe, D. M., 1999, "Thermoelectric, an environmentally friendly source of electrical power," Journal of Renewable Energy, 16 (1-4), pp. 125-6.
[3] Rowe, D. M., and Min, G., 1998, "Evaluation of thermoelectric for power generation." Journal of Power Sources, 73, pp. 193-198.
[4] Min, G., and Rowe, D. M., 2002, "Recent concepts in thermoelectric power generation." Proc. 21st International Conference on Thermoelectrics, pp. 365-374.
[5] Min, G., and Rowe, D. M., 2002, "Symbiotic application of thermoelectric conversion for fluid preheating/power generation," Journal of Energy Conversion and Management, 43, pp. 221-228.
[6] Chen, J., and Wu, C., June 2000, "Analysis on the performance of a thermoelectric generator," Journal of Energy Resources Technology, 122, pp.61-63.
[7] Chen, M., Lu, S., and Liao, B., March 2005 "On the figure of merit of thermoelectric generators" Journal of Energy Resources Technology, 127, pp. 37-41.
[8] Min, G., Rowe, D. M., 1995, "Peltier devices as generators", CRC Handbook of Thermoelectrics, Rowe, D. M., eds., CRC Press, London, pp. 479, Chap. 38.
[9] Lau, P. G., and Buist, R. J., 1997, "Calculation of thermoelectric power generation performance using Finite Element Analysis," Proc. 16th International Conference on Thermoelectrics, pp. 563-566.
[10] Meydbray, Y., Singh, R., and Shakouri, A., 2005, "Thermoelectric module construction for low temperature gradient power generation," Proc. International Conference on Thermoelectrics, pp. 348-351.
[11] Chen, J., March 1996, "Thermodynamic analysis of a solar-driven thermoelectric generator," Journal of Applied Physics, 79(5), pp. 2717-2721.
[12] Khattab, N. M., and El Shenawy, E. T., 2006, "Optimal operation of thermoelectric cooler driven by solar thermoelectric generator" Journal of Energy Conversion and Management, 47, pp. 407-426.
[13] Duffie, J. A., and Beckman, W. A., 1991, Solar Engineering of Thermal Processes, Wiley Interscience, Chap. 7.
[14] Stine, W. B., and Geyer, M., 2001, "Power from the Sun" http://www.powerfromthesun.net/Chapter9/Chapter9new.htm, Chap. 9.
[15] Kreith, F., and Kreider, J. E., 1978, Principles of Solar Engineering, Hemisphere Publishing Corp., Chap. 4.
[16] Melcor, http://www.melcor.com/thermtec.html.
[17] Yazawa, K., Solbrekken, G. L., and Bar-Cohen, A., 2005, "Thermoelectric powered convective cooling of microprocessors," IEEE Transactions on Advanced Packaging, 28(2), pp. 231-239.
[18] Angrist, S. W., 1965, Direct Energy Conversion, Allyn and Bacon, Inc. Chap. 4.
[19] Goldsmid, H. J., 1995, "Conversion efficiency and figure of merit," CRC Handbook of Thermoelectrics, CRC Boca Raton, FL, pp. 19-25.
[20] Kline, S. J., and McClintock, F. A., 1953, "Describing Uncertainties in Single-Sample Experiments," Mechanical Engineering, 75, pp. 3-8.